

# A $^{57}\text{Fe}$ Mössbauer study of black coring phenomena in clay-based ceramic materials

K. J. D. MacKENZIE, C. M. CARDILE\*  
*Chemistry Division, DSIR, Private Bag, Petone, New Zealand*

The black discoloration sometimes found in the interior cores of iron-containing clay-based ceramic materials was studied in three different samples by X-ray diffraction, elemental analysis and  $^{57}\text{Fe}$  Mössbauer spectroscopy. The primary cause of black coring (locally reducing conditions in the interior of the body resulting from incomplete oxidation of carbonaceous impurities) results in the formation of  $\text{Fe}^{2+}$ , but, contrary to previous suggestions, the presence of discrete lower iron oxides or iron metal was not confirmed in the present samples. Instead, the  $\text{Fe}^{2+}$  was found to occur as a lattice substituent of the normal products of the high-temperature ceramic reactions (as ferroan pyroxenes, olivines or feldspars, depending on the chemical composition and reaction conditions). Thus, in the present materials, the dark core reflects the deeper colour of these ferrous minerals, which are not present in the oxidized material of the outer rim.

## 1. Introduction

Black coring is a defect sometimes found in heavy clayware ceramics, and is characterized by a greyish-black coloration of the interior material. The primary cause of black coring has long been recognized as the incomplete burning-out of carbonaceous material, which can produce a coke-like residue [1]. Preoccupation with this aspect of black coring has led to a number of studies of oxidation kinetics [2] and of the effects of heating time and temperature on the rate of carbon burn-out [3, 4]. However, studies of coring in iron-containing clays suggest that in these materials the dark core colour is due more to reduced iron species than to carbon residues [5]. Reduction of the iron compounds can result either from the highly reducing conditions in the vicinity of the unburnt carbonaceous material [5], or, in low-carbon clays, by thermal dissociation of  $\text{Fe}_2\text{O}_3$  to  $\text{FeO}$  and  $\text{O}_2$  at higher temperatures [6]. Black coring is more prevalent where the permeation of oxidizing gas into the sample is hindered, for example, by the formation of glass which blocks the pore structure. The presence of sulphides in the clay appears not to participate in the formation of black cores, but affects the rate of oxidation once the cores are formed [6]. The presence of water vapour arising from thermal decomposition of the clay mineral has been reported to suppress black coring by reacting with the carbon and removing it as  $\text{CO}$  and  $\text{H}_2$  [7].

Various forms of reduced iron have been reported in black-cored materials; magnetite or metallic iron were found by Brownell [5] in various cores in which the amount of residual carbon was too small to account for the dark colour. Metallic iron was also reported by Wakamatsu *et al.* [8] in red clay bodies fired under reducing conditions.

The aim of the present work was to study the nature

and oxidation state of the iron in black-cored clay ceramic bodies using  $^{57}\text{Fe}$  Mössbauer spectroscopy. The study included both conventional ceramic bodies and bodies in which finely-ground glass was deliberately introduced, to investigate its effect on the behaviour of the iron in the core.

## 2. Experimental procedure

Three ceramic bodies were used in the coring studies: I, a commercial yellow-firing sewer pipe body; II, a commercial whiteware body; III, an experimental body composed of 71% New Zealand fireclay, 14% red-firing New Zealand clay and 15% window glass, ground to pass a 100-mesh screen. The chemical and mineralogical analyses of the unfired bodies are presented in Table I.

Bodies I and II were fired in air in an electric laboratory kiln, after extrusion into rods of 30 mm fired diameter. The glass-containing body III was factory-fired in the form of extruded tiles 280 mm  $\times$  280 mm  $\times$  25 mm in an open-flame natural gas kiln operating under oxidizing conditions. Bodies I and II were fired at 900°C for 0.5 h, and body III was fired at 1030°C with an 8 h dwell time at this temperature (total firing time 24 h).

The fired samples were sectioned and the core material dissected out for mineralogical phase analysis using a Phillips PW 1700 automatic computer-controlled X-ray diffractometer with  $\text{CoK}\alpha$  radiation and a graphite monochromator. The room-temperature Mössbauer spectra, obtained using an Elscint AME50 spectrometer, were computer-fitted to Lorentzian lineshapes using a non-linear regression  $\chi^2$  minimization procedure. The velocity scale was referenced to soft iron. Energy dispersive X-ray spectrometry (EDAX) was used to monitor differences in chemical

\*Present address: Alcoa of Australia Ltd, Kwinana, Western Australia 6167, Australia.

TABLE I Chemical and mineralogical analyses of the raw materials for black coring studies

Component	Sewer pipe body I (%)	Whiteware body II (%)	Experimental body III (%)
SiO <sub>2</sub>	53.40	60.21	50.39
Al <sub>2</sub> O <sub>3</sub>	22.55	25.09	24.03
Fe <sub>2</sub> O <sub>3</sub>	7.66	2.04	5.64
MgO	1.96	1.67	2.07
CaO	0.45	0.31	0.81
TiO <sub>2</sub>	1.48	0.94	1.46
Na <sub>2</sub> O	1.75	2.33	2.43
K <sub>2</sub> O	1.26	2.16	2.04
Ignition loss	9.50	5.20	10.80
Total	100.01	99.95	99.67

Mineralogical components			
	Body I	Body II	Body III
	disordered kaolinite	kaolinite	kaolinite
	quartz	quartz	quartz
	mica (tr)	feldspar	crystalite
	amphibole (tr)	mica (tr)	mica (tr)
		talc (tr)	feldspar (tr)
			siderite

tr = trace.

composition between the core and rim material, with differences in carbon content being monitored by proton microprobe analysis.

### 3. Results and discussion

#### 3.1. Mineralogical composition of the cores

The mineralogical compositions of the cores and rims of the three fired materials, determined by X-ray diffraction, are shown in Table II, from which the following points emerge.

1. In most respects, the mineralogical content of each core and its adjacent rim material is identical, except for the following instances:

(i) the core material of body III contains a significant amount of a spinel with an X-ray pattern corresponding most closely to ringwoodite, the spinel form of ferroan forsterite, (Mg,Fe)<sub>2</sub>SiO<sub>4</sub> (JCPDS card no. 21-1255). This spinel is not found in the adjacent rim;

(ii) the core of whiteware body II contains a small amount of ferroan enstatite, (Mg,Fe)SiO<sub>3</sub> (JCPDS card No. 19-605), probably resulting from thermal decomposition of the talc originally present;

(iii) the rim material of the two samples of high iron content (I and III) contains significant amounts of haematite, Fe<sub>2</sub>O<sub>3</sub>, which does not occur in any of the cores.

2. By contrast with previously-reported results [5, 8], no lower-valency iron oxides or metallic iron could be detected by XRD in the black cores of any samples.

3. The only other differences between the core and rim constituents are found in the region of the feldspar XRD reflections (0.29 to 0.33 nm), in which up to five peaks of similar spacing but varying intensity are observed (Fig. 1).

These variations may be understood in terms of different proportions of the following phases: low albite feldspar, NaAlSi<sub>3</sub>O<sub>8</sub> (peaks d and e in Fig. 1, JCPDS card no. 9-466); a high albite feldspar modified by heating (peaks b and c, JCPDS card no. 9-478); and

ferrous enstatite (peaks a and e, JCPDS card no. 19-605).

In the sewer-pipe body I, the chief difference between the core and rim material is the almost complete absence of albite feldspar in the rim material (Fig. 1a).

In the whiteware body II the rim material contains no ferrous enstatite, but relatively more low albite than the core, as evinced by an enhancement of peak d (Fig. 1b).

In the experimental glass-containing body III, the differences between the rim and core material lie mainly in the relative proportions of high and low albite present, the core containing a greater proportion of peak c corresponding to high albite (Fig. 1c).

Thus, rather than occurring as discrete lower oxide phases, the reduced iron of the core material appears to be associated with some of the minerals which are formed as a result of the normal thermal reaction processes of the body, and in some cases may even influence the phases which are formed, e.g. as in the ferrous spinel phase in core III and the ferrous enstatite in core II, in which Fe<sup>2+</sup> may be exerting a stabilizing effect. In addition to ringwoodite and ferrous enstatite, two other phases present in these cores could also act as hosts for Fe<sup>2+</sup>; these are feldspars (especially the calcian plagioclases, in which Fe<sup>2+</sup> can proxy to a limited extent for Ca<sup>2+</sup> [9]) and mullite, Al<sub>6</sub>Si<sub>2</sub>O<sub>13</sub>, of which a small amount was detected in the core of body III. The mullite structure readily accepts Fe<sup>3+</sup> [10], but on reduction, ferrous mullite can be formed, evinced by a characteristic Mössbauer spectrum [11].

The essential similarity of the mineral suite in the core and rim regions of each of the present samples is further supported by EDAX analyses of the elemental compositions; although the sample texture made it difficult to obtain representative analyses, the results revealed no systematic compositional differences between the core and rim material of each sample. Likewise, proton microprobe analysis of the carbon content of the glass-containing body III showed no

Figure 1 Part of the X-ray traces of the black core samples, with their respective rims, in the region of the major feldspar/pyroxene reflections, with line diagrams from the JCPDS powder data file for comparison. (a) Sewer pipe body I, (b) whiteware body II, (c) experimental glass-containing body III.

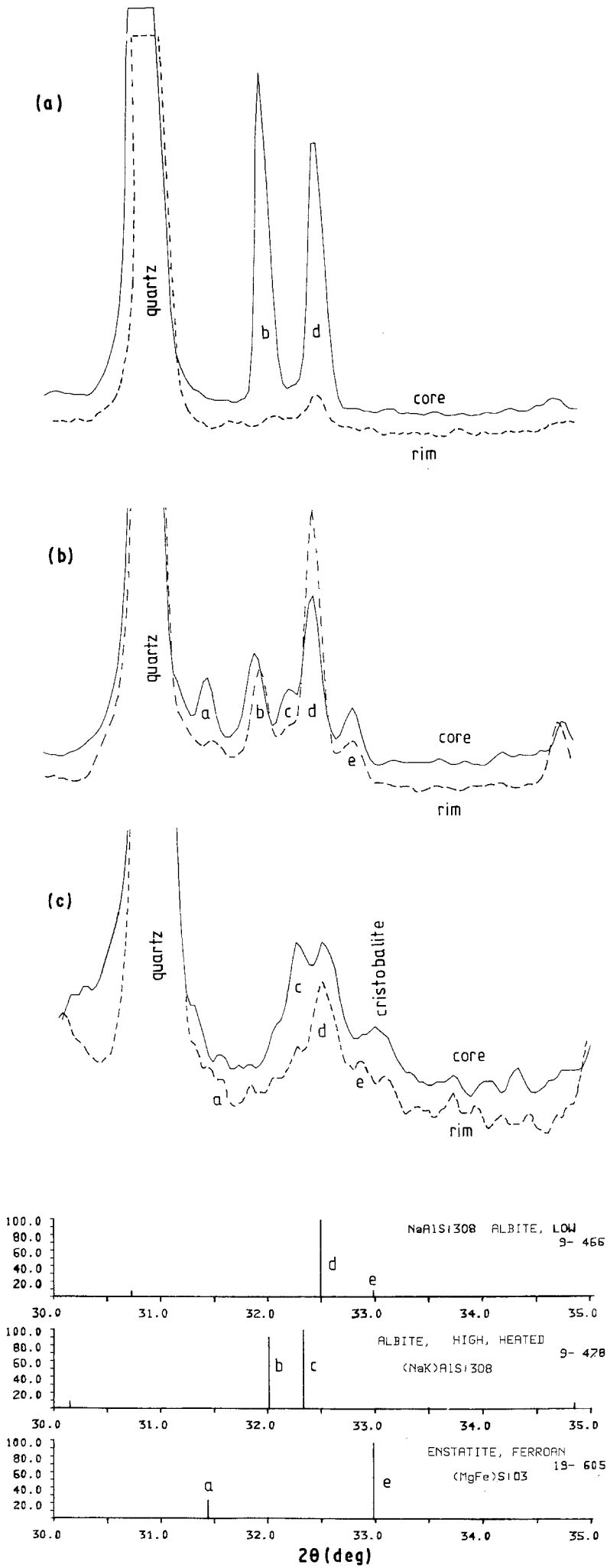


TABLE II Minerological contents of the core and rim material of the three fired ceramic bodies

Body	Core	Rim
Sewer pipe body I	quartz (major) feldspar amphibole (tr)	quartz (major) feldspar amphibole (tr) haematite
Whiteware body II	quartz (major) feldspars mica dehydroxylate (tr) ferroan enstatite (tr)	quartz (major) feldspars mica dehydroxylate (tr)
Experimental body III	quartz (major) cristobalite (major) feldspars ferroan ringwoodite mullite (tr)	quartz (major) cristobalite (major) feldspars haematite

tr = trace.

significant differences between the core and the rim material, suggesting that elemental carbon is not the source of the colour in that sample.

### 3.2. Mössbauer spectroscopy

The room-temperature Mössbauer spectrum of the experimental body III before firing (Fig. 2a) is best fitted by four quadrupole doublets, the parameters of which are given in Table III. Comparison with the Mössbauer spectra of the two clays and the glass component which compose the body indicate that its spectrum arises from the fireclay, in which doublets a and b have parameters typical of  $\text{Fe}^{3+}$  in octahedral sites, doublet d is typical of octahedral  $\text{Fe}^{2+}$ , and doublet c arises from a siderite ( $\text{FeCO}_3$ ) impurity.

After firing, a number of concentric haloes could be distinguished around the black core; these range in colour from yellow at the outermost rim, becoming progressively darker brown towards the inner core.

The material from each halo was separately investigated by Mössbauer spectroscopy, but all were found to have similar spectra which could best be fitted to three quadrupole doublets (Table III). The isomer shifts (IS) and quadrupole splittings (QS) of doublets e and f are very similar to the values found for the major  $\text{Fe}^{3+}$  resonances in mullite (IS = 0.28 to 0.37  $\text{mm sec}^{-1}$ , QS = 1.17 to 1.30  $\text{mm sec}^{-1}$ ; IS = 0.28 to 0.38  $\text{mm sec}^{-1}$ , QS = 0.63 to 0.92  $\text{mm sec}^{-1}$  [10]). The absence of a well-defined mullite XRD pattern in the rim material of this sample suggests that the observed Mössbauer spectrum arises from an incipient mullite phase on the point of recrystallization. Doublet g corresponds to the inner pair of a magnetically-split six-line haematite spectrum. A slight but progressive increase in the relative intensity of the haematite spectrum was observed in the darker inner haloes. Measurements of the spacing of the complete haematite spectrum indicate an internal field ( $B_{\text{eff}}$ ) of

TABLE III Room-temperature Mössbauer parameters of black cored sample sand related materials. The isomer shifts (IS) are quoted with respect to natural iron.

Sample	Doublet	IS ( $\text{mm sec}^{-1}$ )	QS ( $\text{mm sec}^{-1}$ )	Width ( $\text{mm sec}^{-1}$ )	Area (%)	Phase
Experimental body III (unfired)	a	0.27	0.86	0.51	40.3	fireclay
	b	0.36	0.48	0.26	11.8	fireclay
	c	1.24	1.81	0.28	29.4	fireclay
	d	1.29	2.43	0.39	18.4	siderite
Experimental body III (fired, outer rim)	e	0.30	1.01	0.53	49.6	mullite
	f	0.31	0.58	0.39	39.2	mullite
	g	0.48	2.62	0.32	11.2	haematite
Experimental body III (fired, black core)	a	0.26	0.94	0.30	3.6	fireclay
	b	0.35	0.47	0.41	3.3	fireclay
	h	1.35	2.26	0.50	6.9	ringwoodite?
	i	0.85	1.30	0.70	49.9	ringwoodite?
	j	0.95	2.08	0.47	25.7	plagioclase
	k	1.10	1.28	0.38	10.7	plagioclase
Sewer pipe body I (fired, black core)		0.29	0.45	0.33	3.2	fireclay?
	j	0.93	2.02	0.53	29.5	plagioclase
	k	0.93	1.19	0.68	28.2	plagioclase
	l	1.13	2.11	0.46	16.7	enstatite
	m	1.10	2.73	0.45	17.9	enstatite
	n	0.53	0.53	0.35	4.6	enstatite
Whiteware body II (fired, black core)	l	1.05	2.05	0.53	32.5	enstatite
	m	1.10	2.57	0.53	29.2	enstatite
	n	0.43	0.43	0.44	3.4	enstatite
	o	0.98	1.55	0.74	34.9	enstatite

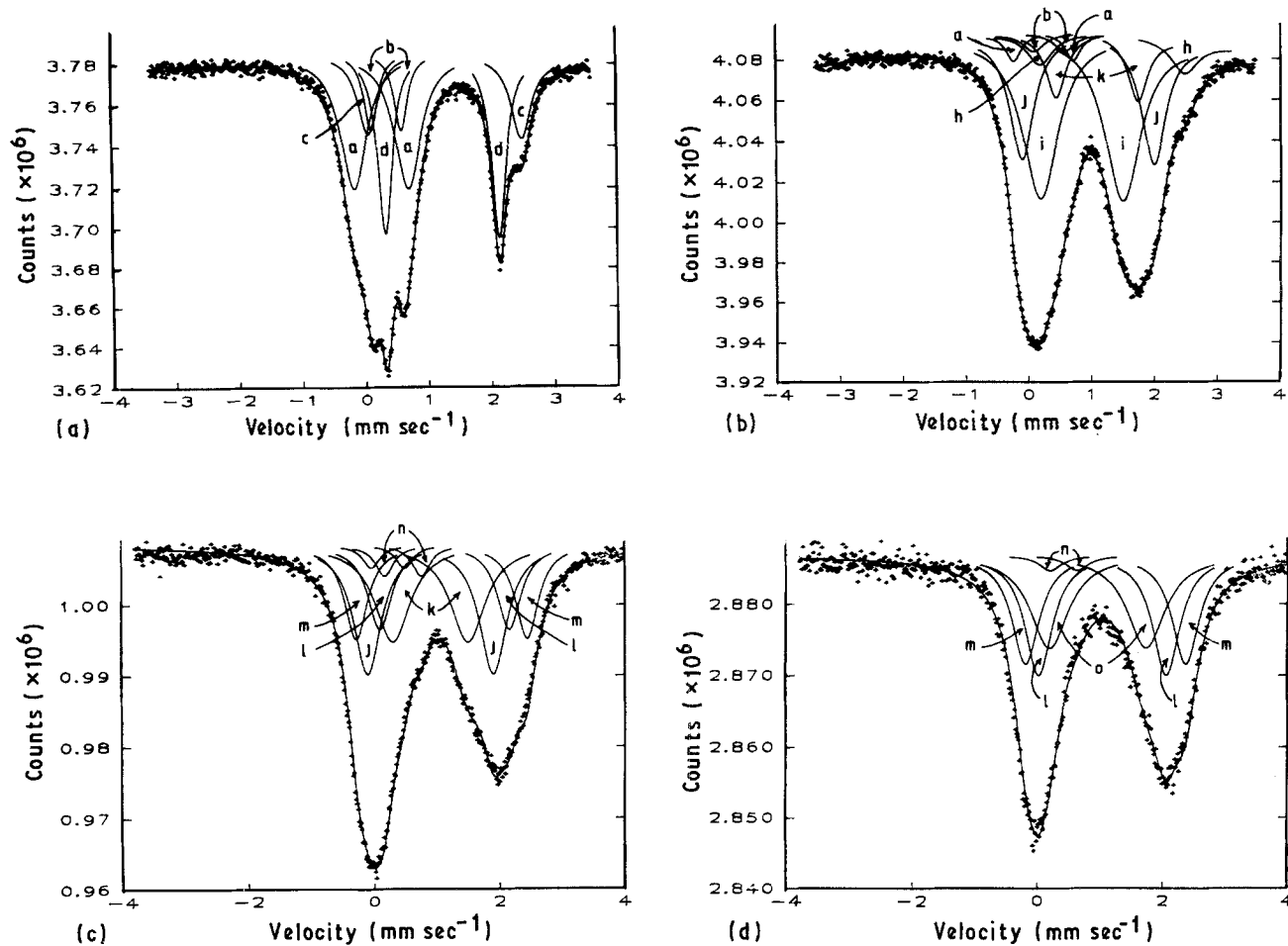


Figure 2 Room-temperature Mössbauer spectra of black core samples and related materials. (a) Experimental body III, unfired; (b) experimental body III, black core; (c) sewer pipe body I, black core; (d) whiteware body II, black core.

51.2T, suggesting little or no substitution of  $Al^{3+}$  for  $Fe^{3+}$ .

By contrast, the Mössbauer spectrum of the core of sample III is quite different ( Fig. 2b), requiring six quadrupole doublets for a statistically satisfactory fit (Table III). The low-intensity doublets a and b have parameters corresponding to the similarly labelled doublets in the unheated material, indicating that the thermal reactions in this region of the sample are not fully complete, at least as far as the iron constituent is concerned. Of the remaining four resonances, two (doublets j and k, Table III) correspond with the parameters reported for iron in plagioclase feldspar ( $IS = 0.90$  to  $0.92$   $mm\ sec^{-1}$ ,  $QS = 1.54$  to  $1.55$   $mm\ sec^{-1}$ ;  $IS = 1.13$  to  $1.14$   $mm\ sec^{-1}$ ,  $QS = 2.01$  to  $2.13$   $mm\ sec^{-1}$  [12, 13]).

Doublets h and i may belong to the other major iron-containing phase known to be present in this sample (ringwoodite,  $(Mg,Fe)_2SiO_4$ ), for which Mössbauer data do not appear to have been reported previously. However, the parameters of i and j are somewhat similar to two of the resonances reported for a closely related structure, ferroan spinel,  $(Mg,Fe)Al_2O_4$  ( $IS = 0.63$  to  $0.86$   $mm\ sec^{-1}$ ,  $QS = 1.88$  to  $2.24$   $mm\ sec^{-1}$ ;  $IS = 0.85$  to  $0.86$   $mm\ sec^{-1}$ ,  $QS = 0.86$  to  $1.23$   $mm\ sec^{-1}$  [14]). Thus it seems reasonable to attribute doublets h and i to a spinel phase such as ringwoodite.

The Mössbauer spectra of the cores from bodies I and II are shown in Figs 2c and d, and the parameters listed in Table III. The spectra from cores I and II,

although not identical, show similarities with the core spectrum from body III. The spectrum of sewer pipe body core I contains, in addition to a low-intensity  $Fe^{3+}$  doublet which is probably a residual from the original clay mineral, five other doublets, two of which (j and k) are similar to the plagioclase resonances identified in core III above. Two other doublets (l and m, Table III) have parameters similar to those reported for ferroan enstatite ( $IS = 1.09$   $mm\ sec^{-1}$ ,  $QS = 2.64$   $mm\ sec^{-1}$ ;  $IS = 0.92$  to  $1.12$   $mm\ sec^{-1}$ ,  $QS = 1.85$  to  $1.96$   $mm\ sec^{-1}$  [15, 16]). In addition to these reported enstatite resonances, two other resonances have been reported in a closely related series of pyroxenes ( $IS = 0.41$  to  $0.60$   $mm\ sec^{-1}$ ,  $QS = 0.36$  to  $0.66$   $mm\ sec^{-1}$ ;  $IS = 1.13$  to  $1.18$   $mm\ sec^{-1}$ ,  $QS = 1.45$  to  $2.02$   $mm\ sec^{-1}$  [17]); the parameters of doublet n (Table III) compare well with the first of these resonances. Thus, the Mössbauer spectrum of the black core from body I suggests that the iron resides predominantly in the feldspar and pyroxene phases.

The Mössbauer spectrum of the black core from whiteware body II (Fig. 2c, Table III) is best fitted to four doublets with parameters typical of enstatite/pyroxene, again suggesting that the ferrous iron is located in the silicate product phase and not in discrete lower iron oxides or iron metal. The colour of these cores must therefore result from the presence of ferroan silicate phases rather than from lower iron oxides as previously suggested. Although every core sample contains at least one resonance with parameters similar to those of ferrous mullite ( $IS = 1.00$   $mm$

$\text{sec}^{-1}$ ,  $QS = 2.06 \text{ mm sec}^{-1}$  [11]), all the spectra can be explained without invoking this phase; the available evidence neither conclusively supports nor rules out the presence of  $\text{Fe}^{2+}$  in mullite.

The presence of deliberately introduced glass does not appear to alter the behaviour of the iron in the black cores significantly, apart from possibly modifying the suite of product phases, which reflect the bulk composition of the body. No evidence was found in the present work for changes in the mechanisms of the firing reactions attributable to sealing of the pores by the molten glass.

#### 4. Conclusions

1. The colour of the black cores in three different iron-containing clay-based ceramic bodies appears to be due to the presence of  $\text{Fe}^{2+}$  resulting from locally reducing conditions in the centre of the body.

2. Although the oxidized outer rim of the body can contain  $\text{Fe}_2\text{O}_3$  the presence of discrete lower iron oxides in the core regions was not observed, either by X-ray diffraction or by Mössbauer spectroscopy. Thus, the black colour appears not to be due to lower oxides or metallic iron, as has been previously suggested.

3. The main differences noted between the mineralogical contents of the oxidized outer rims of the samples and the dark-coloured cores were:

(i) the presence of haematite,  $\text{Fe}_2\text{O}_3$ , in the outer rims of the two most iron-rich samples but not in the cores;

(ii) the presence of ferrous minerals such as ferroan enstatite,  $(\text{Mg,Fe})\text{SiO}_3$  and ferroan ringwoodite,  $(\text{Mg,Fe})_2\text{SiO}_4$  in some of the cores but not in their corresponding rims;

(iii) differences in the amounts and/or types of feldspars present both in the cores and rims.

4. The Mössbauer spectra of the cores suggest that the reduced iron species are present as substituents of the feldspar minerals as well as the pyroxene and spinel-type olivine (ringwoodite).

5. Because the carbon contents of the rims and cores are identical and no significant systematic differences

in chemical composition were detected between the rims and cores of the samples, the colour of the cores appears to be due to the dark colour of the ferroan minerals. This situation is not changed by the presence of additional glass in the sample.

#### Acknowledgements

We are indebted to Mr G. V. White for providing the samples, to Mrs K. Card for the EDAX analyses, to Dr I. Vickridge for the carbon analyses, and to Dr I. W. M. Brown for discussion of the X-ray analyses.

#### References

1. H. SALMANG, in "Ceramics - Physical and Chemical Fundamentals" (Butterworth, London, 1961) p. 117.
2. P. S. NICHOLSON and W. A. ROSS, *J. Amer. Ceram. Soc.* **53** (1970) 154.
3. C. BARDIN and J. SALOME, *Terre Cuite* **44** (1970) 27.
4. C. BEARDMORE and R. W. FORD, *Trans. J. Brit. Ceram. Soc.* **85** (1986) 101.
5. W. E. BROWNELL, *J. Amer. Ceram. Soc.* **40** (1957) 179.
6. P. FISCHER, *Ceram. Forum Int./Ber. DKG* **60** (1983) 322.
7. J. E. HOUSEMAN, R. A. PERKINS and C. J. KOENIG, *Bull. Amer. Ceram. Soc.* **47** (1968) 1138.
8. M. WAKAMATSU *et al.*, *Yogyo Kyokai Shi* **93** (1985) 349.
9. W. A. DEER, R. A. HOWIE and J. ZUSSMAN, in "An Introduction to the Rock Forming Minerals" (Longmans, London, 1966) p. 298.
10. C. M. CARDILE, I. W. M. BROWN and K. J. D. MacKENZIE, *J. Mater. Sci. Lett* **6** (1987) 357.
11. C. M. CARDILE and M. E. BOWDEN, *Mater. Sci. Forum* **34-36** (1988) 611.
12. D. E. APPLEMAN *et al.*, Proceedings of the 2nd Lunar Science Conference, Vol. 1, edited by A. A. Levinson (Massachusetts Institute of Technology, Cambridge, 1971) p. 117.
13. S. S. HAFNER, D. VIRGO and D. WARBURTON, *Earth Planet. Sci. Lett.* **12** (1971) 159.
14. I. W. M. BROWN and C. M. CARDILE, unpublished data.
15. B. O. MYSEN, F. A. SEIFERT and D. VIRGO, *Amer. Mineral* **65** (1980) 867.
16. S. MITRA, *Neues Jahrb. Mineral. Monatsh* (1976) 169.
17. G. N. GONCHAROV, S. B. TOMILOV and A. S. SHAROV, *Zap. Vses. Mineral. O-va* **106** (1977) 215.

Received 15 February

and accepted 16 August 1989